Rubidium Isotope Effect in Superconducting Rb_3C_{60}

B. Burk, Vincent H. Crespi, A. Zettl, and Marvin L. Cohen
Department of Physics, University of California at Berkeley, Berkeley, California 94720
and Materials Sciences Division, Lawrence Berkeley Laboratory, Berkeley, California 94720
(Received 14 February 1994)

We have measured the resistive superconducting transition temperature in C_{60} single crystals intercalated with isotopically pure ^{87}Rb and ^{85}Rb and with natural abundance rubidium. We obtain a rubidium isotope effect exponent of $\alpha_{Rb} = -0.028 \pm 0.036$, a result which implies that the Rb-C_{60} optic phonons play at most a minor role in the pairing mechanism of Rb_3C_{60}.

PACS numbers: 74.70.Wz, 63.20.Kr, 74.25.−q

The detailed mechanism of superconductivity in alkali-intercalated C_{60} remains controversial, with proposals for both electronic [1,2] and phonon-mediated [3–8] mechanisms. The phonon mechanism can be further subdivided into models that rely exclusively upon on-ball molecular phonons [3–5] and those which incorporate additional modes such as librons [8], translational modes [9], or alkali-C_{60} optic phonons [6,7]. For any superconducting mechanism, we can write $T_c \propto M_i^{-\alpha_i}$, where M_i is the mass of a given atomic constituent and α_i is the isotope shift exponent for this atomic species. Although these models generally predict a carbon isotope effect, a substantial intercalant isotope effect is expected only for models with a significant alkali-C_{60} optic phonon contribution to the pairing mechanism. An accurate measurement of the alkali atom isotope effect would therefore provide a useful constraint on the mechanism of superconductivity.

To date, isotope effect measurements on A_3C_{60} (A = K, Rb) consist of a single rubidium experiment [10] and several carbon isotope effect experiments [11–15]. There is uncertainty concerning the intrinsic carbon isotope effect in that a more homogeneous carbon isotopic distribution seems to yield a smaller carbon isotope effect [16]. The most complete substitution to date yields $\alpha_C = 0.3 \pm 0.05$ for K_3C_{60} and Rb_3C_{60} [16]. Susceptibility measurements on powder samples of T_c have yielded an upper limit on the rubidium isotope effect exponent of $\alpha_{Rb} < 0.2$ [10]. Comparing the T_c's of K_3C_{60} and Rb_3C_{60} *at equal lattice constant* does not constitute a valid alkali isotope experiment. Since $T_c^{Rb_3C_{60}} > T_c^{K_3C_{60}}$ at equal lattice constant [17], such an approximation would suggest an inverse isotope effect of rough magnitude $\alpha_{alk} \approx -0.2 \pm 0.2$. However, this result is clouded by the large difference in ionic radii between K and Rb, which could yield a change in vibrational dynamics of the same magnitude as that caused by the change in alkali mass. Considering the present experimental situation, a greater certainty in α_{Rb} is desirable in order to narrow the constraints on plausible pairing mechanisms. We report detailed measurements of the effect of rubidium isotope substitution on the resistive T_c in C_{60} single crystals doped with ^{85}Rb, ^{87}Rb, and natural abundance rubidium, ^{nat}Rb.

Single-crystal C_{60} samples (typically 1 mm × 1 mm × 0.1 mm) were intercalated with rubidium vapor following the technique developed by Xiang *et al.* [18]. Since isotopically pure elemental rubidium is not commercially available, we produced all rubidium used in this experiment by extraction of Rb metal from RbCl. We extract rubidium metal from isotopically enriched RbCl (RbCl at 99.2% ^{87}Rb, 0.8% ^{85}Rb and RbCl at 99.8% ^{85}Rb, 0.2% ^{87}Rb from U.S. Services) and from natural abundance RbCl (RbCl at 72.2% ^{85}Rb, 27.8% ^{87}Rb from Aldrich). Our independent mass spectroscopy measurements verify the manufacturer's isotopic composition to within 1%. We place 177 mg RbCl and approximately 500 mg finely divided calcium into a Pyrex tube which is continuously evacuated by a mechanical pump. The RbCl and calcium mixture at one end of the tube is heated with a flame until the mixture reacts (near the melting point of RbCl, $\approx 718\,^\circ$C). The reaction produces rubidium vapor and $CaCl_2$. The rubidium vapor rapidly condenses on the cool portion of the tube wall away from the reacting mixture. After reaction completion, the open end of the tube is sealed with a flame and the tube segment with condensed rubidium metal is separated in a glove box and introduced into the intercalation vessel.

We note that the procedure outlined here differs from that described by Ebbesen *et al.* [10]. They reacted lithium with RbCl to liberate rubidium. Initially, we used an independently developed lithium reaction method but found separation of rubidium from residual lithium to be difficult. With the calcium reaction, separation is trivial since the calcium vapor pressure is 3 to 4 orders of magnitude lower than the rubidium vapor pressure over a wide temperature range. Heating the reaction products with a flame drives the rubidium vapor away from the remaining calcium.

In Fig. 1 we show resistance versus temperature data of ^{85}Rb, ^{87}Rb, and ^{nat}Rb intercalated samples near T_c, normalized to the resistance at $T = 32$ K. The resistive transitions are sharp (for this material), indicating a high degree of homogeneity within a given sample. We define T_c by the maximum in the derivative of the resistance with respect to temperature. Figure 2 shows dR/dT for each sample. The data are fitted with a cubic spline, and the maximum of the fit determines T_c (parabolic and Gauss-

0031-9007/94/72(23)/3706(4)$06.00

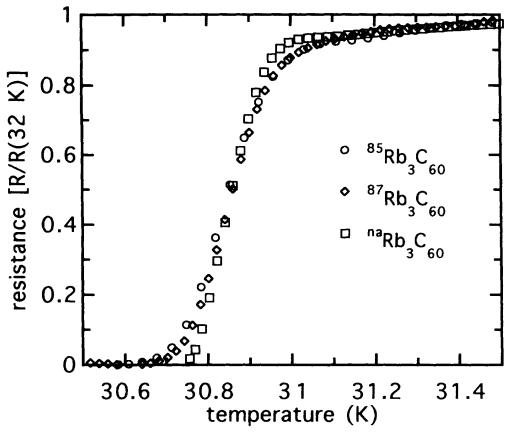

FIG. 1. Normalized resistance versus temperature near T_c for $^{85}Rb_3C_{60}$, $^{87}Rb_3C_{60}$, and $^{nat}Rb_3C_{60}$.

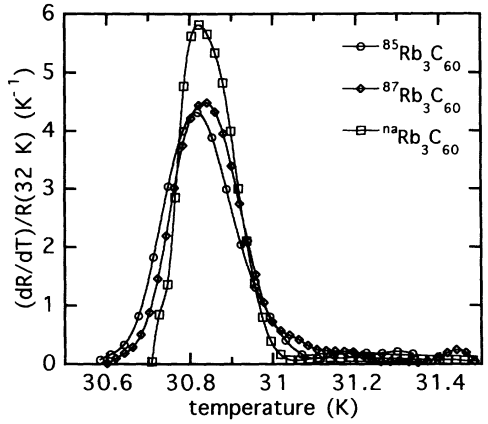

FIG. 2. Derivative with respect to temperature of normalized resistance near T_c for $^{85}Rb_3C_{60}$, $^{87}Rb_3C_{60}$, and $^{nat}Rb_3C_{60}$. Curves are cubic spline fits to the data. Position of curve fit maximum determines T_c.

ian fits yield essentially equivalent results). We measured the resistive transitions several times, T_c being reproducible to within 5 mK for a given sample. We define the width of the transition as the separation between the maximum and minimum in the second derivative, yielding transition widths from 140 to 180 mK. Although the transition for $^{nat}Rb_3C_{60}$ appears to be slightly narrower, the range of variation in transition width observed in natural abundance samples encompasses the results for the isotopically pure samples. We assign an uncertainty in T_c of 0.1 times the transition width. This uncertainty estimate is always greater than the reproducibility spread of T_c for a given sample; it reflects our estimate of the errors introduced by inhomogeneous broadening of the transition.

Before presenting the isotopically shifted results, we note that our measurements provide the most accurate determination to date for T_c in Rb_3C_{60}. For $^{nat}Rb_3C_{60}$ we find $T_c = 30.82 \pm 0.09$ K, where the uncertainty reflects possible temperature sensor calibration errors. This result is 1–2 K higher than reported susceptibility measurements of T_c [11,19] and about 0.6 K higher than previous resistive T_c's [20]. We have verified that temperature gradients between the sample and the temperature sensor (Lakeshore CGR2000) are small. We have measured resistance curves for a sample vessel immersed in a sealed container with liquid neon in which the neon vapor pressure and the temperature sensor provide simultaneous temperature measurements. The temperature sensor calibration agrees with the neon vapor pressure-derived temperature to within 90 mK. Furthermore, the measured T_c (as determined by the temperature sensor) is independent of whether or not the sample vessel is immersed in liquid neon, indicating that the temperature lag between sample and sensor is negligible in the normal measurement configuration without the neon.

Figure 3 displays our results for T_c measured in $^{85}Rb_3C_{60}$, $^{87}Rb_3C_{60}$, and $^{nat}Rb_3C_{60}$. The data are plotted as T_c versus average rubidium mass. For comparison we plot the result for the BCS maximum value of $\alpha_{Rb} = 0.5$ normalized to the $^{87}Rb_3C_{60}$ data point. We obtain $\alpha_{Rb} = -0.028 \pm 0.036$, or equivalently $\Delta T_c = -20 \pm 26$ mK for $^{87}Rb_3C_{60} \rightarrow {}^{85}Rb_3C_{60}$ (the error bars indicate the 65% confidence interval). To within our experimental uncertainty there is no rubidium isotope effect on T_c in Rb_3C_{60}.

Before discussing the implications of this result for the different pairing mechanisms, we consider an indirect rubidium isotope effect due to a weak dependence of lattice constant on Rb mass. Both electronic [2] and phonon-mediated mechanisms are expected to exhibit an effect of lattice constant on transition temperature. To estimate this effect, we use the experimentally determined lattice constant dependence of T_c, 44 KÅ^{-1} [17,18]. The isotopic shift in lattice constant can be estimated from the fractional change in crystal isotopic mass $\Delta M/M$, the bulk modulus B, the phonon mode energies E_i, and

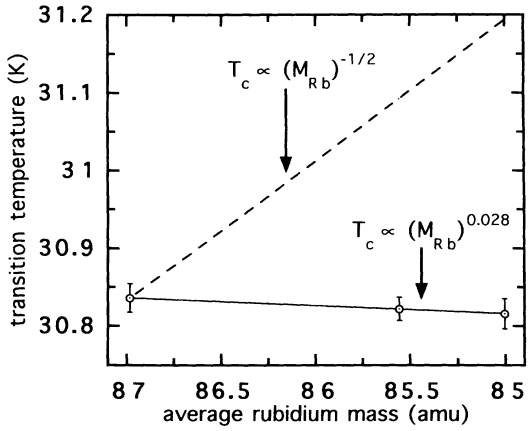

FIG. 3. Plot of T_c versus average rubidium mass in Rb_3C_{60}. Solid line is fit of the data by $T_c \propto M_{Rb}^{0.028}$. Dashed line shows $T_c \propto M_{Rb}^{-1/2}$ with proportionality constant chosen so that the line passes through the $^{87}Rb_3C_{60}$ data point.

Grüneisen constant γ_i [21],

$$\frac{\Delta a}{a} = -\frac{2}{3}\frac{\Delta M}{M}\frac{1}{Ba^3}\sum \gamma_i E_i . \quad (1)$$

We treat the C_{60} molecule as a single entity, yielding four "atoms" per unit cell. The relevant phonon frequencies are the intermolecular translational and Rb-C_{60} optic modes, with frequencies in the range 50–300 K. An upper limit on the Grüneisen constants can be estimated from the pressure dependence of the bulk modulus [17], which provides information about the hardening of the intermolecular modes with pressure. These estimates yield $\Delta a \approx (0.5\text{–}2.0)\times 10^{-4}$ Å for $^{87}Rb_3C_{60} \rightarrow {}^{85}Rb_3C_{60}$, which translates into an increase in T_c of 2–9 mK. The entire range of this estimate falls within 2 standard deviations of the experimental result for α_{Rb}, indicating that the null experimental result is robust under consideration of isotopic shifts in lattice constant.

In addition to increasing the lattice constant, the substitution of ^{85}Rb for ^{87}Rb could harden the librational potential, reducing a possible librational contribution to the electron-phonon coupling. Such an effect can be estimated from the dependence of the librational mode frequency upon the size of the alkali atom [22]. The substitution of Rb for K increases the librational frequency by 8 K. The steric effects of this substitution also increase the lattice constant by 0.15 Å. The $^{87}Rb \rightarrow {}^{85}Rb$ substitution increases the lattice constant by $(0.5\text{–}2.0)\times 10^{-4}$ Å, implying a tiny increase in librational mode frequency on the order of 10^{-2} K, a negligible effect.

A model of superconductivity in Rb_3C_{60} incorporating both on-ball carbon phonons and Rb-C_{60} optic modes would predict a direct rubidium isotope effect due to isotopic shift in phonon frequency. The present experiment places limits on the relative contributions of rubidium modes within such a model. First we obtain a simple analytic constraint on the relative contribution of rubidium modes to the electron-phonon coupling. We assume that T_c depends on atomic mass only through the mass dependence of the average phonon frequency,

$$\alpha_i = \frac{1}{2}\frac{d\ln T_c}{d\ln\omega_{\log}}\frac{d\ln\omega_{\log}^{-2}}{d\ln M_i}, \quad (2)$$

where $\omega_{\log}$ is defined by

$$\omega_{\log} = \exp\left(\sum_n \frac{\lambda_n}{\lambda}\ln\omega_n\right), \quad (3)$$

with λ_n the electron-phonon coupling constant to the mode with frequency ω_n and λ is the total coupling constant. The logarithmic frequency average is the most accurate single-frequency approximation for the full spectrum of electron-phonon coupling. Using the McMillan formula for T_c [23] with a spectrum of pure carbon and Rb-C_{60} optic modes, we obtain

$$\frac{\alpha_{Rb}}{\alpha_C+\alpha_{Rb}}\frac{3M_{Rb}}{M_{eff}} = \frac{\lambda_{Rb}}{\lambda}, \quad (4)$$

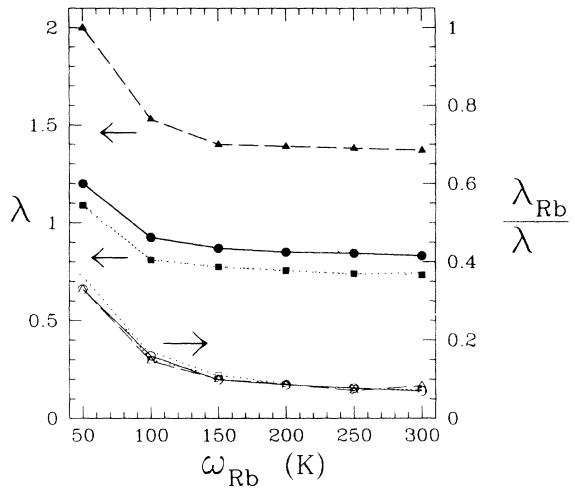

FIG. 4. Total electron-phonon coupling strength λ (upper curves, solid symbols) and upper bound on the ratio of Rb-C_{60} optic mode coupling strength to total coupling λ_{Rb}/λ (lower curves, open symbols) as a function of alkali mode frequency for three theoretical models of the on-ball electron-phonon coupling. The values of λ_{Rb}/λ plotted yield $\alpha_{Rb}=0.044$, the experimentally determined upper bound on the rubidium isotope effect. Dotted curves refer to the model of Varma, Zaanen, and Raghavachari [3] which has the fitted value $\mu^*=0.16$. Solid curves refer to the model of Schluter *et al.* [5] ($\mu^*=0.17$). Dashed curves refer to the model of Jishi and Dresselhaus [4] ($\mu^*=0.23$).

where $M_{eff}=3M_{C_{60}}M_{Rb}/(M_{C_{60}}+3M_{Rb})$ is an estimate of the effective optic mode mass. The contribution to α_C from the weak Rb mass dependence of the carbon modes has been neglected. An upper bound on α_{Rb} yields an upper bound on the fractional contribution of λ_{Rb} to λ. Using the minimal reported value for α_C ($\alpha_C=0.3$ [11]) and 2 standard deviations above the measured α_{Rb} as an upper bound on α_{Rb} ($\alpha_{Rb}<0.044$), this simple analytic model yields $\lambda_{Rb}/\lambda<0.17$. Adjusting for a possible lattice-constant-induced isotope shift of 2–9 mK would decrease this bound by roughly 10%.

In order to examine the effects of the detailed frequency distribution of the electron-phonon coupling we performed numerical solutions of the Eliashberg equations for various electron-phonon coupling spectra. The on-ball carbon phonons were modeled following the results of three theoretical calculations [3–5]. The frequency of the Rb-C_{60} optic modes was varied from 50 to 300 K. Neutron scattering results suggest mode frequencies on the order of 200 K [24], while theoretical treatments [6,25] place these modes in the range from 50 to 200 K. For each electron-phonon coupling spectrum the values of λ, μ^*, and λ_{Rb} were varied to match experimental constraints of $\alpha_C=0.3$, $T_c=30.8$ K, and $\alpha_{Rb}<0.044$. The results are presented in Fig. 4. The three models yield different values of λ and μ^* while the limits on λ_{Rb}/λ remain essentially unchanged. As the frequency of the alkali modes increases from 50 to 300 K, the limit on

λ_{Rb}/λ decreases from 0.33 to 0.08 for all three spectra. Although the contribution of the alkali modes to T_c is at best small, the contribution of a low-frequency alkali mode to λ can be substantial. In contrast to the analytic model, the ratio λ_{Rb}/λ is only weakly dependent on α_C. Decreasing (increasing) the carbon isotope effect exponent to 0.2 (0.4) results in significantly increased (decreased) values of λ and μ^*, but the ratio λ_{Rb}/λ decreases (increases) by only 10%. This reduced sensitivity to α_C is due to the great disparity between the alkali and carbon phonon frequencies. Modifying the electron-phonon coupling spectrum by the addition of substantial coupling to a low-frequency librational mode at 50 K [8] yields a limit on λ_{Rb}/λ roughly 10% larger. In all cases, removal of the maximal allowed alkali-C_{60} optic mode contribution to the coupling function results in a reduction in T_c of 1–4 K, indicating that the alkali modes make at most a minor contribution to T_c.

Although the estimated uncertainty in T_c yields a value of isotope exponent consistent with $\alpha_{Rb}=0$, the actual data points hint at a small inverse isotope effect. An inverse isotope effect is well known for hydrogen at the octahedral interstitial sites of the fcc Pd lattice [26]; it has been interpreted within the framework of anharmonic phonons [27]. Anharmonicity of the alkali vibration in the A_3C_{60} system could conceivably depress or even invert the isotopic signature of the alkali modes, weakening the limit on λ_{Rb}/λ.

In summary, we have made precise measurements of T_c in isotopically substituted Rb_3C_{60} which yield a null result for the rubidium isotope effect in Rb_3C_{60}. This result puts stringent limits on the possible contributions of alkali-C_{60} optic phonons to the superconductivity.

We thank Michael Fuhrer for producing the C_{60} crystals used in this work. This work was supported by National Science Foundation Grants No. DMR-90-17254 (B.B. and A.Z.) and No. DMR-9120269 (V.H.C. and M.L.C.), and the Director, Office of Energy Research, Office of Basic Energy Sciences, Materials Sciences Division of the U.S. Department of Energy under Contracts No. DE-AC03-76SF00098 (B.B. and A.Z.) and No. DE-AC03-76SF00098 (V.H.C. and M.L.C.).

[1] S. Chakravarty, M. P. Gelfand, and S. Kivelson, Science **254**, 970 (1991).
[2] S. Chakravarty, S. A. Kivelson, M. K. Salkola, and S. Tewari, Science **256**, 1306 (1992).
[3] C. M. Varma, J. Zaanen, and K. Raghavachari, Science **245**, 989 (1991).
[4] R. A. Jishi and M. S. Dresselhaus, Phys. Rev. B **45**, 2597 (1992).
[5] M. Schluter, M. Lannoo, M. Needles, and G. A. Baraff, Phys. Rev. Lett. **68**, 526 (1992).
[6] F. C. Zhang, M. Ogata, and T. M. Rice, Phys. Rev. Lett. **67**, 3452 (1991).
[7] G. H. Chen, Y. J. Guo, N. Karasawa, and W. A. Goddard III, Phys. Rev. B **48**, 13959 (1993).
[8] I. I. Mazin, O. V. Dolgov, A. Golubov, and S. V. Shulga, Phys. Rev. B **47**, 538 (1993).
[9] A crude estimate of the electron-phonon coupling strength for intermolecular translational modes can be found in V. H. Crespi, J. G. Hou, X.-D. Xiang, M. L. Cohen, and A. Zettl, Phys. Rev. B **46**, 12064 (1992).
[10] T. W. Ebbesen, J. S. Tsai, K. Tanigaki, H. Hiura, Y. Shimakawa, Y. Kubo, I. Hirosawa, and J. Mizuki, Physica (Amsterdam) **203C**, 163 (1992).
[11] C.-C. Chen and C. M. Lieber, J. Am. Chem. Soc. **114**, 3141 (1992).
[12] A. P. Ramirez, A. R. Kortan, M. J. Rosseinsky, S. J. Duclos, A. M. Mujsce, R. C. Haddon, D. W. Murphy, A. V. Makhija, S. M. Zahurak, and K. B. Lyons, Phys. Rev. Lett. **68**, 1058 (1992).
[13] T. W. Ebbesen, J. S. Tsai, K. Tanigaki, J. Tabuchi, Y. Shimakawa, Y. Kubo, I. Hirosawa, and J. Mizuki, Nature (London) **355**, 620 (1992).
[14] A. A. Zakhidov, K. Imaeda, D. M. Petty, K. Takushi, H. Inokuchi, K. Kikuchi, I. Ikemoto, S. Suzuki, and Y. Achiba, Phys. Lett. A **164**, 355 (1992).
[15] P. Auban-Senzier, G. Quirion, D. Jerome, P. Bernier, S. Della-Negra, C. Fabre, and A. Rassat, Synth. Met. **56**, 3027 (1993).
[16] C.-C. Chen and C. M. Lieber, Science **259**, 655 (1993).
[17] O. Zhou, G. B. M. Vaughan, Qing Zhu, J. E. Fischer, P. A. Heiney, N. Coustel, J. P. McCauley, and A. B. Smith III, Science **255**, 833 (1992).
[18] X.-D. Xiang, J. G. Hou, G. Briceño, W. A. Vareka, R. Mostovoy, A. Zettl, V. H. Crespi, and M. L. Cohen, Science **256**, 1190 (1992).
[19] G. Sparn and J. D. Thompson, Phys. Rev. Lett. **68**, 1228 (1992).
[20] X.-D. Xiang, J. G. Hou, V. H. Crespi, A. Zettl, and M. L. Cohen, Nature (London) **361**, 54 (1993).
[21] H. Holloway, K. C. Hass, M. A. Tamor, T. R. Anthony, and W. F. Banholzer, Phys. Rev. B **44**, 7123 (1991).
[22] D. A. Neumann, J. R. D. Copley, D. Reznik, W. A. Kamitakahara, J. J. Rush, R. L. Paul, and R. M. Lindstrom (unpublished).
[23] W. L. McMillan, Phys. Rev. **167**, 331 (1968).
[24] J. W. White, G. Lindsell, L. Pang, A. Palmisano, D. S. Silva, and J. Tomkinson, Chem. Phys. Lett. **191**, 92 (1992).
[25] W. Zhang, H. Zheng, and K. H. Bennemann, Solid State Commun. **82**, 679 (1992).
[26] B. Stritzker and W. Buckel, Z. Phys. **257**, 1 (1972).
[27] V. H. Crespi and M. L. Cohen, Solid State Commun. **83**, 427 (1992).